Ionization of heavy ions and (atomic) products of nuclear reactions in various media

N. K. Skobelev

Joint Institute for Nuclear Research, Dubna

Fiz. Elem. Chastits At. Yadra **20**, 1439–1478 (November–December 1989)

Processes of heavy-ion ionization in the passage through gaseous and solid targets are studied. A review is given of the experimental and theoretical studies on the charge distributions of heavy ions at the exit from the target as a function of the target thickness (x) and atomic number (Z_t). The mean charges of ionized atoms produced by knockout from the target in nuclear reactions involving heavy ions differ significantly from the values predicted by semiempirical equations when the atomic number of the product (Z_p) is larger than 50. The processes accompanying the passage of heavy ions through matter are described.

INTRODUCTION

In passing through a medium, heavy ions[1)] in ion–atom collisions undergo charge fluctuations owing to electron capture or stripping processes.

Study of the changes in heavy-ion charge states due to electron capture or loss is interesting because these data can serve as an important source of information about the nature of atomic collisions. Many theoretical problems in ion–atom collisions have been studied in the monographs of Refs. 1 and 2. It is possible in principle to describe collisions of such complicated systems if the ion–electron and ion–ion interaction potentials are known. However, it is still impossible to obtain an exact description in practice.

In many model studies of ion–atom interactions, the electrons of the incident ion and target atoms are split into two groups: the electrons of the outer shells (the outer electrons) and those of the inner shells (the inner electrons or electrons of the ion core).

In most cases of the practical study of atomic processes it is necessary to deal with multiply charged heavy ions having many electrons in the outer and inner shells, the interaction with which leads to heavy-ion charge exchange.

In fact, in addition to interactions between the heavy ion and electrons of the target atoms, interactions can occur between the heavy ion and the ion core of the target atoms.[3]

In crystals such collisions lead to knockout of the core from lattice sites and the appearance of point defects.[4] The interaction of heavy ions with the electrons and ion core of the target atoms also leads to loss of electrons or electron excitation, and also to ion bremsstrahlung.

Knowledge of the charge-exchange cross sections for heavy ions in a medium and their charge states and energy loss is necessary for many practical problems.

Let us list a few of these.

In the design of heavy-ion accelerators it is necessary to estimate the ion loss during the acceleration process using data on the cross sections for ion charge-exchange on residual gases.

In the construction of heavy-ion sources and multistage accelerators it is necessary to have data on the energy loss and charge distribution occurring in the passage through the gas-filled region or solid charge-exchange target as a function of the heavy-ion velocity.

For the implantation of semiconducting materials it is necessary to know the charge content of the heavy-ion beams.

The interaction of a high-temperature plasma with the walls of a thermonuclear reactor cannot be estimated without knowledge of the ion charge-exchange cross sections.

Owing to the importance of these problems, a large number of studies have been carried out on the charge-exchange cross sections of heavy ions, and also on the charge distribution of heavy ions in passing through gaseous or solid targets in various energy ranges.

Let us mention a few of the most interesting studies which have been carried out on this problem.

The experimental data (obtained before 1972) on the charge distribution of heavy ions passing through gaseous or solid targets was collected by Wittkower and Betz.[5] The more recent data summarized by Shima[6] refer to the charge distribution of heavy ions after their passage through thin foils.

The studies of Nikolaev,[7,8] Betz,[9] and Delaunay[10] were devoted to the detailed analysis of the latest experimental data on the charge states of heavy ions at the exit from various media.

The most complete survey of the experimental data on the cross sections for heavy-ion charge exchange and their analysis is given in the review of Betz.[9]

Interest in the ion charge states of fission fragments first arose in connection with the study of relations between the mean free path and the energy (velocity) of a fragment. To calculate the fragment energy loss it was necessary to compute the ion charges of the fragment for all velocities in the deceleration process. Such calculations were carried out by Bohr[11] and Lamb,[12] and the first results on the measurement of heavy-ion charges were obtained by Lassen.[13] They measured the fragment charges in gaseous and solid absorbers.

From the above we see that quite a long time has passed since the appearance of these studies. New results and approaches to understanding ionization processes have appeared during this time. New studies have begun, and a number of features in the ionization of nuclear-reaction products have been discovered.

In this review we mainly concentrate on the charge distribution of heavy ions and atoms of nuclear-reaction products at the exit from the target medium.

The author has attempted to include as much as possible of the new information on this question.

 0090-4759/89/060613-18$04.40

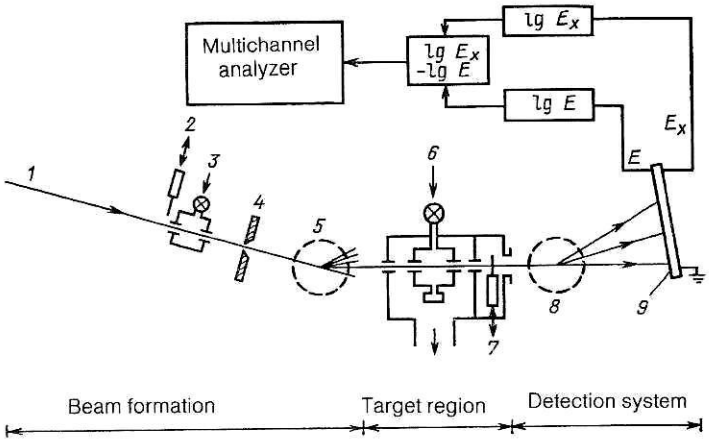

FIG. 1. Experimental setup used to measure the charge states with gaseous and solid targets: 1—monoenergetic beam of accelerated ions; 2—charge-exchange solid foil; 3—gas-filled volume; 4—collimator; 5—selector for separating a given ion charge (q_i); 6—gaseous target with a system for regulating its thickness; 7—a set of solid targets of various thicknesses; 8—ion charge-state analyzer; 9—position-sensitive device for detecting fractions of charge states.

1. EXPERIMENTAL TECHNIQUES FOR STUDYING CHARGE STATES

The experimental setups used to study the charge states of heavy ions in their passage through gaseous or solid targets have been described in Refs. 7, 9, and 14. In Fig. 1 we schematically show the principal elements of the setup used with various modifications to measure the charge states of heavy ions.[9,14]

Wide-band magnetic analyzers[15,16] are the most convenient device for analyzing the charge states of heavy ions and nuclear-reaction products leaving or knocked out of a solid target into a vacuum region. The scheme for one such setup is shown in Fig. 2. All these setups contain three principal elements:

1. An accelerator with a system for transporting beams of heavy ions of a given charge.

2. A device with a target (a "stripper") consisting of an evacuated volume containing a thin gaseous target or a device for setting up a thin solid target in the form of a self-supporting foil in the path of the ion beam.

3. A detection system containing, as a rule, a magnetic spectrometer for analyzing the charge distribution of a beam leaving a target with various charge components and a position-sensitive detection device for determining the relative strengths of these charge states with information collection and processing.

Gas-filled magnetic separators have been used to measure the mean charge of heavy ions or ionized products of nuclear reactions involving heavy ions in a gaseous medium.[17,18] At the present time new gas-filled universal separators are being introduced to study the products of nuclear reactions involving heavy ions. The use of these separators broadens our knowledge of the ionization processes of atoms and nuclear-reaction products.

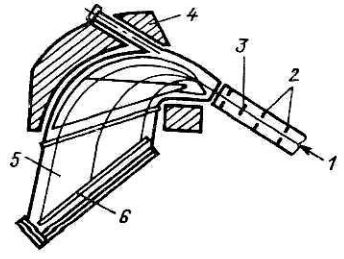

FIG. 2. Scheme for measuring charge states using a magnetic analyzer: 1—ion beam; 2—collimator system; 3—solid target; 4—yolk of the magnetic analyzer; 5—vacuum chamber; 6—position-sensitive detector for recording charge states of heavy ions.

2. EXPERIMENTAL DATA ON THE CHARGE STATES OF HEAVY IONS IN MATTER AND THEIR ANALYSIS

As already mentioned above, Bohr[11] made an important contribution to the description of the charge states of fission fragments in atomic collision processes, taking into account electron loss and capture by heavy fragments. Regarding the mean charge, Bohr assumed that heavy ions passing through rarefied gases retain those electrons which have orbital velocity higher than the ion velocity. The electrons with smaller velocities are lost in collisions. Losses of electrons with higher velocities are of low probability. The collisions for such electrons are adiabatic. In accordance with this criterion (henceforth referred to as the Bohr criterion), we assume "slow" those particles or ions whose velocities are small in comparison with the orbital velocities (u) of the electrons of that particle ($v_p \ll u$). When $v_p > u$, the ions are termed "fast." The Bohr criterion serves as the basis for practically all the recent theoretical and empirical studies of the charge-exchange process.

The Lamb treatment,[12] for example, differs from that of Bohr in that the orbital velocity u was taken to be the quantity $u = (2I_i/m)^{0.5}$, where I_i is the binding energy of the outer electron in the ion.

Of greatest interest from the viewpoint of charge-exchange processes are heavy ions whose velocities (v_p). lie in the range $v_0 < v_p < z_p v_0$, where v_0 is the electron velocity in the hydrogen atom, referred to as the Bohr velocity, and is equal to $e^2/\hbar = 2.188 \cdot 10^8$ cm/sec. In other words, this means that we consider strongly ionized atoms, which, however, still contain many electrons in the inner shells.

When an ion with charge q passes through a gaeous target, it collides with the atoms or molecules and can capture or lose one or more electrons in each collision with a probability expressed as $\sigma(q, q')$, referred to as a cross section (q and q' are the ion charge before and after a collision with change of the charge by one unit, and σ is expressed in units of cm^2/atom or cm^2/molecule).

The charge distribution of the ion beam varies with the thickness of the gaseous target x. These variations obey the

system of equations

$$dF_q(x)/dx = \sum_{q'(q \neq q')} [\sigma(q', q) F_{q'}(x) - \sigma(q, q') F_q(x)], \quad (1)$$

which describe the competition between electron capture and loss. The quantity $F_q(x)$ is the fraction of ions with charge $q(\Sigma_q F(q) = 1)$. The target thickness (x) is given by the expression[19] $x = 3.35 \times 10^{16} LP$ mol/cm^2 for $t = 15$ °C, where L is expressed in cm and P is in mn Hg.

In principle, q can vary in the range $-1 \leqslant q \leqslant Z_p$. For ions with relatively high velocities, the fraction of charges with $q = -1$ is small and can be neglected.

There exist theoretical models for the calculation of the cross section for the capture or loss of a single electron by a heavy ion.[9]

According to Bohr,[11,20] for heavy ions in light targets (small Z_t) the cross section for electron loss σ_l is given by

$$\sigma_l = 4\pi a_0 Z_p^{1/3} Z_t^2 (v_0/v_p)^3, \quad (2)$$

while the capture cross section is

$$\sigma_c = 4\pi a_0 Z_p^{1/3} Z_t^5 (v_0/v_p)^6, \quad (3)$$

where $a_0 = \hbar^2/m_e e^2 = 5.29 \times 10^9$ cm (the Bohr radius of the atom), Z_p is the ion atomic number, and Z_t is the target atomic number.

For ions passing through heavy targets the cross sections for electron capture and loss are given by the symmetric expression

$$\sigma_c = \sigma_l \simeq \pi a_0^2 (Z_p^{1/3} + Z_t^{1/3}) (v_0/v_p)^2. \quad (4)$$

There are a number of other theoretical calculations of the cross sections, and also empirical relations for estimating them.[8,21,22]

Knowledge of the capture cross sections and electron loss of heavy ions interacting with matter is necessary for estimating the equilibrium thickness of a charge-exchange foil or a gaseous target.

Betz and Schmelzer[23] made rough estimates of the charge- exchange cross sections in air for all ions up to uranium as a function of the velocity and charge of the ion q. However, to estimate σ it is necessary to know the mean equilibrium charge $\bar{q}$, defined as

$$\bar{q} = \sum_q qF(q). \quad (5)$$

In the case of a symmetric distribution the mean equilibrium charge coincides with the most probable value of the charge.

The rest of our discussion will be concerned only with the equilibrium charge states $\bar{q}$ of heavy ions, in connection with the calculation or measurement of these quantities on the basis of the ionization of heavy ions in a medium.

These values are often the same as the effective charges (q_{ef}) determined from the energy losses of heavy ions in passing through matter. We note that for heavy-ion energies of about 1 MeV/nucleon and higher, these values do not always coincide. Questions of q_{ef} are therefore discussed in the Appendix.

According to the Bohr criterion,[11] the mean equilibrium charge of heavy ions of a given energy can be estimated on the basis of the losses in the target of part of the orbital electrons of the moving particle. This reduces the problem of calculating $\bar{q}(v_p, Z_p)$ to the calculation of the velocity of the orbital electrons of the ion, $u(Z_p, q_i)$. In the derivation of an analytic expression for this dependence, the electron velocity $u = Z^* v_0/\nu^*$ is introduced, where Z^* is the measured field strength in the region where the electrons are bound, and ν^* is the so-called "effective" quantum number. The quantity Z^* corresponds approximately to the number of electrons with velocities smaller than u, i.e., $Z^* \simeq \bar{q}$, and $u \simeq v_p$. It can then be concluded that $\bar{q} \simeq \nu^* v_p/v_0$.

Bohr showed that for most freely coupled electrons in the ground state of the ion the statistical Thomas–Fermi model for a large intermediate range of charges ν^* has a maximum at a value close to $Z_p^{1/3}$ (when q is no larger than $Z_p/2$). This approximation was used to obtain the expression

$$\bar{q}/Z_p = v_p/(v_0 Z_p^{2/3}) \quad \text{for} \quad 1 < v_p/v_0 < Z_p^{2/3}. \quad (6)$$

In the first approximation this expression reflects the behavior of $\bar{q}$ in rarefied gases.

In the passage of slow heavy ions through a gas, with the exception of hydrogen, the highest value of $\bar{q}$ is obtained for the gases N_2, O_2, and Ar with only a small difference between them.[9] For heavier gases at the same ion velocities $\bar{q}$ decreases slightly with increasing atomic number of the gas (Z_t).

In the passage of ions of the same energy through solid targets $\bar{q}$ has higher values than for gases, while the tendency for $\bar{q}$ to decrease with increasing Z_t is the same. Beryllium and carbon proved to be very effective targets for charge exchange. The poorest targets are those of gold and metals with similar Z. This behavior is also manifested for fast ions with relatively small Z_p (Refs. 9 and 14).

In the passage of slow ions through hydrogen the equilibrium charge depends strongly on the ion velocity. As the energy increases $\bar{q}$ grows and becomes comparable with the values of $\bar{q}$ in N_2, O_2, etc.[9]

In most of the noble gases and especially in helium the mean equilibrium charge manifests an unusual behavior. Relatively light ions passing through helium can acquire the highest value of $\bar{q}$ in gases, where these values can be close to those obtained for ions with solid targets. At higher ion velocities the anomalous effects disappear and helium becomes a relatively ineffective "stripper."

In Fig. 3 we compare the theoretical and experimental data for the mean charges of heavy ions in the range $16 \leqslant Z_p \leqslant 92$ which have passed through regions containing the gases N_2 and O_2 and air.

Other approximations and statistical methods for calculating the average equilibrium charge states of ions were later developed.

3. SEMIEMPIRICAL EXPRESSIONS FOR CALCULATING THE MEAN EQUILIBRIUM CHARGE STATES OF HEAVY IONS

Various semiempirical expressions for calculating $\bar{q}$ have been derived on the basis of the observed trends in the behavior of the charge distributions of ions at the exit from a target.

The first analytic semiempirical relation for $\bar{q}$ was obtained by Dmitriev and Nikolaev[24] in 1964. On the basis of

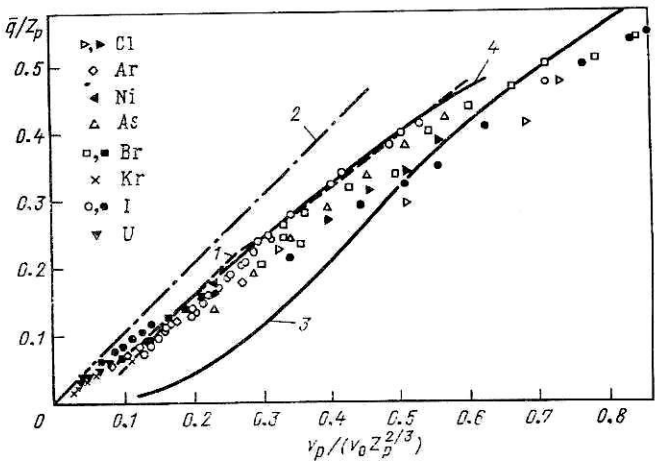

FIG. 3. Theoretical and experimental results for the relative equilibrium ionization $\bar{q}/Z_p$ of heavy ions which have passed through gaseous targets of nitrogen, oxygen, and air as functions of the reduced velocity $v_p/(v_0 Z_p^{2/3})$. The experimental values are shown as points. The curves correspond to theoretical estimates from the following sources: 1—Lamb (Ref. 12); 2—Bohr (Ref. 11); 3—Brunings *et al.* (for large Z_p) (Ref. 22); 4—Bell (Ref. 21).

the Thomas–Fermi model and the experimental data, these authors assumed that the speed of the orbital electrons in an ion is $u \simeq Z_p^{\alpha} f(q/Z_p)$, where α is some parameter.

Application of the Bohr criterion to this expression for u led to the following expression for the mean charge of an ion in gases:

$$\bar{q}/Z_p = \lg [(v_p/m_1)\, Z_p^{\alpha_1}]/\lg (n_1 Z_p^{\alpha_2}) \qquad (7)$$

in the range $0.3 \leqslant \bar{q}/Z_p \leqslant 0.9$.

The four parameters α_1, α_2, m_1, and n_1 (Table I) are extracted from comparison with the experimental distributions of the charge states of ions with $Z_p \leqslant 10$ and fission fragments.

The error in reproducing $\bar{q}$ was $\sim 5\%$. For $\bar{q}/Z_p < 0.3$ a different empirical relation was suggested:

$$\bar{q}/Z_p = A v_p Z_p^{-1/2}.$$

The parameter is $A \sim 0.18$ for ion charge exchange in nitrogen and hydrogen.

The authors attempted to use this relation to determine the mean charge of heavy ions passing through thin solid targets. In this case the parameter A was taken to be ~ 0.33. For the range $0.3 \leqslant \bar{q}/Z_p \leqslant 0.9$ other values of the coefficients were also suggested ($\alpha_1 = 0.1$, $\alpha_2 = 0.6$, $m_1 = 1.2$, and $n_1 = 5.0$). However, these equations have not been widely used.

Later, Betz *et al.*[25] proposed a different semiempirical relation for the mean charge states:

$$\bar{q}/Z_p = 1 - C \exp [-v_p/(v_0 Z_p^{\gamma})], \qquad (8)$$

where the parameters C and γ were determined empirically and varied, depending on the type of ion and medium through which the ions pass.

In Table II we list the values of these parameters for the passage of ions through air and Formvar.

For heavy ions with $v_p \geqslant v_0$. in gaseous targets (in particular, oxygen, air, and argon) the choice of the constants $C \simeq 1$ and $\gamma = 2/3$ gave reasonable values for $\bar{q}$, which differed from the experimental values in a wide range of Z_p by less than 2 units of charge. It should be noted that at the present time estimates of the mean charges for heavy ions at the exit from gaseous targets are made on the basis of the Bohr (6) and Betz (8) equations, since they give the best description of the actual $\bar{q}$. These formulas also lead to satisfactory agreement for the mean values of the charges of ionized products of nuclear reactions knocked out into a gaseous medium. However, for heavy ions and nuclear reaction products in the region of the rare-earth elements, Petrov *et al.*[17] discovered that shell effects in atoms strongly affect the mean charge of heavy ions. In air and helium the values of $\bar{q}$ for ion velocity ratio in the range $v_p/v_0 \sim 3$–4 turned out to be 15% or more below the expected value. The authors attributed this anomaly in the behavior of $\bar{q}$ to the decrease of the cross sections for electron loss from the deeper $4f$ shell.

According to the Bohr criterion, the equilibrium charge corresponds to equality of the electron capture cross section σ_c and loss cross section σ_l. Since $\sigma_c \sim q^2$ (Refs. 9 and 20), a decrease of σ_l tends to shift the equilibrium to smaller values of the ion charge. In measurements of the charge states of atomic products of evaporation reactions knocked out into a helium medium, in the range of atomic numbers Z up to 102 (Ref. 18) it was found that the value of the mean charge is decreased also in this region, where ionization of the next $5f$ shell is expected to occur.

In Fig. 4 we show the variation of the equilibrium charges of ions in helium for fixed velocity ratio $v_p/v_0 = 2.2$, obtained from the orthonormalized data of Refs. 17 and 18 as a function of the ion atomic number Z_p. Here we have extrapolated the equilibrium charges of the ionized products of evaporation reactions to ions with larger Z_p.

In this case the fluctuations of the distributions near the equilibrium charge can be estimated as

$$\Delta q_i/q_i \sim 1/k \sqrt{N}\, \Delta q/\bar{q} \quad \text{or} \quad \Delta q/\bar{q} \simeq 0.5\, \Delta I_i/I_i,$$

where N is the number of ion collisions with the target atoms and I_i is the ionization potential of the ith electron.

TABLE I. Values of the parameters in the semiempirical equation (7) for $\bar{q}/Z_p$ as a function of Z_t of the medium.

Medium	α_1	α_2	m_1	n_1
H_2	0.4	0.3	1.2	4.0
He			1.3	4.5
N_2, Ar			0.9	7.0

TABLE II. Values of the parameters C and γ in the semiempirical equation (8) for $\bar{q}/Z_p$ for various ions in air and Formvar.

Ion	Air		Formvar	
	C	γ	C	γ
S	1.135	0.663	1.083	0.604
As	1.117	0.628	1.098	0.538
I	1.065	0.641	1.030	0.518
U	—	—	1.030	0.510

Turning now to estimates of $\bar{q}$ at the exit of solid targets, we note that to obtain agreement between the experimental values of $\bar{q}$ and the estimates using Eq. (8) it is necessary to take into account the decrease of the parameter γ with increasing Z_p of the ion (see Table II). Using the crude approximation for $v_p > v_0$ and $0 < Z_p \leqslant 92$ that γ is a function $f(Z_p)$, Eq. (8) can be transformed[25] to

$$\bar{q}/Z_p = 1 - C\,(0.71 Z_p^{\alpha})^{v_p/v_0}. \qquad (9)$$

For Formvar the parameter is $\alpha = 0.053$, and C is the same as in Table II. More recent experiments with heavy ions at energies above 0.3 MeV/A have indicated that $\bar{q}$ deviates considerably from the calculated values. Nikolaev and Dmitriev[26] took into account the most recent data on the equilibrium ion charge distributions and proposed another semiempirical expression for calculating the mean charge of an ion (for $Z_p \geqslant 16$) in passing through a solid target:

$$\bar{q}/Z_p = [1 + (Z_p^{-\alpha} v_p/v')^{-1/K}]^{-K} = [1 + X^{-1/K}]^{-K}, \qquad (10)$$

where $\alpha = 0.45$, $K = 0.6$, and $v' = 3.6 \times 10^8$ cm/sec. This equation leads to better agreement with the experimental data; in most cases the difference is no more than a single charge state in all cases where the "reduced velocity" is

$$X = v_p/(v' Z_p^{0.45}) = 3.86 \sqrt{\frac{E_p}{A_p}} \Big/ Z_p^{0.45} < 1{,}5. \qquad (A)$$

In Fig. 5 we compare the experimental values of $\bar{q}$ with the values calculated using Eqs. (7), (9), and (10).

To and Drouin[27] made a slight change in the dependence of $\bar{q}$ on the same parameters as in Eq. (10).

$$\bar{q}/Z_p = 1 - \exp[-(v_p/v')\, Z_p^{-0.45}] = 1 - \exp(-X). \qquad (11)$$

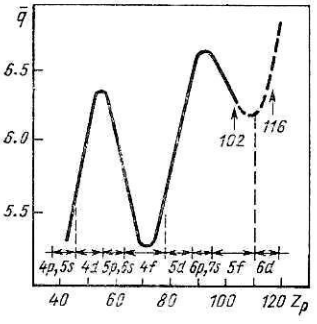

FIG. 4. Mean ion charge $\bar{q}$ of heavy ions (reaction products) with atomic number Z_p and $v_p/c = 1.6\%$ in helium (at pressure 1 mm Hg).

The normalization was made for ions with $Z_p < 18$ and $E_p < 7$ MeV with a carbon target. Baron[28] extended this to higher ion energies $E_p/A_p > 0.068\, Z_p^{0.9}$ (MeV/A), taking the parameter α equal to 0.447:

$$\bar{q}/Z_p = \left[1 - \exp\left(-\frac{3.8585}{Z_p^{0.447}} \sqrt{\frac{E_p(\text{MeV})}{A_p}}\right)\right]. \qquad (12)$$

Sayer[29] also analyzed the ion charge distributions and derived a semiempirical equation for the equilibrium states. His study is interesting for asymmetric distributions, of which more will be said below. Shima *et al.*[30] chose a more universal expression for determining $\bar{q}$ on a carbon target in all ranges of X for $Z_p \geqslant 8$:

$$\bar{q}/Z_p = 1 - \exp(-1.25X + 0.32X^2 - 0.11X^3). \qquad (13)$$

As already noted, the equilibrium charge distributions depend on the atomic number Z_t of the solid medium through which the heavy ion passes.[9]

The experiments of Baron and Delaunay[10,31] showed that the mean equilibrium charge of krypton depends strongly on the type of target. They approximated the variations of the mean equilibrium ion charge in the medium by the equation

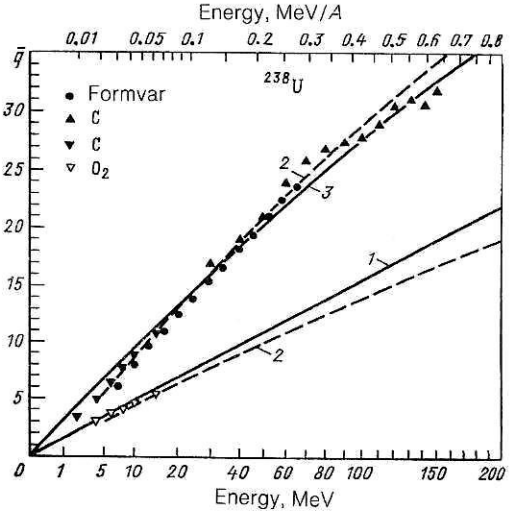

FIG. 5. Mean equilibrium charges of uranium ions which have passed through oxygen, carbon, and Formvar targets as functions of the ion energy (figure borrowed from Ref. 9): calculations using the equations of: 1—Nikolaev (Ref. 24); 2—Betz *et al.* (Ref. 25); 3—Nikolaev and Dmitriev (Ref. 26).

$$\bar{q}_{Z_t} = \bar{q}\,(Z_t = 6)\,[1 - 5.21\cdot10^{-3}\,(Z_t - 6) + 9.56\cdot10^{-5}\,(Z_t - 6)^2 - 5.96\cdot10^{-7}\,(Z_t - 6)^3], \quad (14)$$

where $\bar{q}(Z_t = 6)$ is the average charge of an ion after passing through carbon foil.

Shima *et al.*[30] suggested a different dependence for q_{Z_t} on the atomic number Z_t of a solid target $4 \leqslant Z_t \leqslant 79$ and $E_p < 6$ MeV/A).

$$\bar{q}_{Z_t}/Z_p = \frac{\bar{q}\,(Z_t=6)}{Z_p}\,[1 + g\,(Z_t)], \quad (15)$$

where $g(Z_t) = -0.0019\ (Z_t - 6)\ \sqrt{X} + 10^{-5}\ (Z_t - 6)^2 X$.

Both of these equations give realistic values for $\bar{q}_{Z_t}$ and can be used for estimates if $\bar{q}(Z_t = 6)$ is taken to be the experimental values or values calculated using (10) and (13) in their regions of validity.

However, experiments carried out recently to study the charge distributions up to uranium have shown that for carbon targets of the corresponding thickness, Eqs. (10) and (13) can be used with fairly good accuracy ($\sim$0.5 units of charge) for heavy ions only up to Kr. For ions heavier than Kr the experimental values of $\bar{q}$ are close to the calculated values for ion energies of up to $\sim$1 MeV/A (Fig. 6) (Refs. 15 and 32). At higher energies there are indications that the experimental values of the mean equilibrium charges of the ions ^{132}Xe, ^{197}Au, ^{208}Pb, and ^{238}U are lower than the predictions.[32]

For ^{197}Au ions of energy 352 MeV passing through a thin carbon film ($\sim$80 μg/cm^2), the mean equilibrium charge is 5 units lower than the calculated value (Fig. 7).

We note that for ions of high energy, where it would seem that the ions would be completely stripped, i.e., lose all their electrons, in passing through the target significant discrepancies are observed.

For example, for elastically scattered ^{20}Ne ions of energy 18 MeV/A, after passage through a Ta target not only charge states 10^+, but also states 9^+ are observed (in 7% of the cases) (Ref. 33). In the passage of ^{40}Ar ions of energy

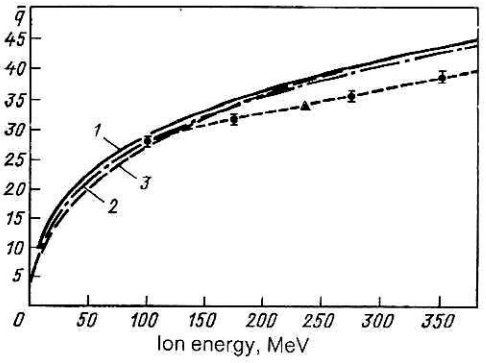

FIG. 7. Values of the mean equilibrium charges $\bar{q}$ of heavy ions ^{197}Au (Ref. 32) which have passed through carbon foil (black circles), and values calculated by Sayer (1), Shima (2), and Nikolaev and Dmitriev (3) as functions of the energy.

11.6 and 18.7 MeV/A through a carbon target,[34] the fraction of charge states 17^+ was 21.6 and 10.5%, respectively.

Experiments carried out at GANIL (in France) in beams of $^{40}Ar^{16+}$ (44 MeV/A) and $^{48}Kr^{35+}$ (33.2 MeV/A) ions showed that these ions also are not completely stripped in passing through thin foils of carbon and gold.[35]

In Tables III and IV we give the data on the distribution of charge states of ^{40}Ar (44 MeV/A) in the passage through carbon and gold targets of various thicknesses.

On the other hand, the picture is dramatically different for the passage of ^{40}Ar ions of energy 44 MeV/A through thick targets of beryllium and gold.[36] After passage through a beryllium target the Ar ions are almost completely stripped, unlike the ions at the exit of a gold target (Table V).

These seemingly contradictory experimental data can be interpreted if it is assumed that at such high ion velocities the condition for single collisions is satisfied in thin solid targets. According to the estimates of Rozet *et al.*,[37] the mean free path between single collisions is 350 μg/cm^2 in carbon and 53 μg/cm^2 in gold. The shakedown effect has a fairly short reponse time ($\tau_w \sim 2\times10^{-16}$ sec).

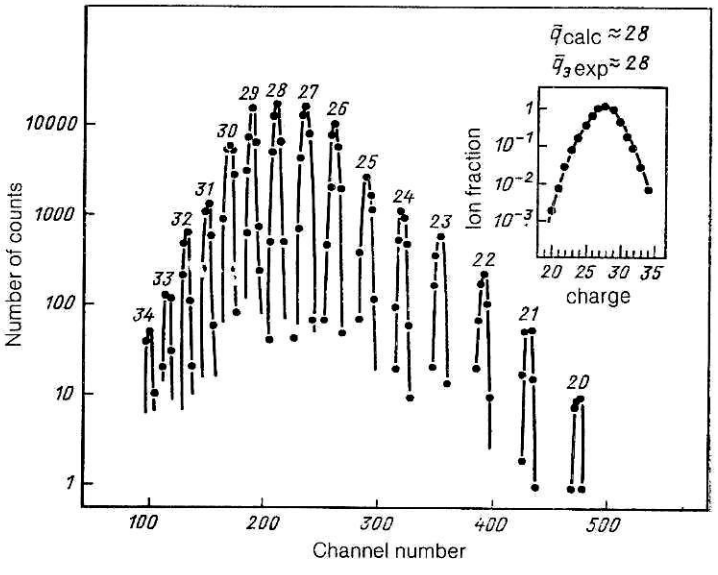

FIG. 6. Charge distribution of ^{136}Xe ions of energy 144 MeV after passing through carbon foil (Ref. 15). The value of $\bar{q}$ was calculated using the equation of Nikolaev and Dmitriev (Ref. 26).

TABLE III. Fraction of charge states (%) of ^{40}Ar (44 MeV/A) at the exit from a thin carbon foil.

Thickness of the carbon foil, $\mu g/cm^2$	Charge state of ^{40}Ar, %		
	16+	17+	18+
100	61	34	5
250	27	45	28
450	5	39	56

The anomalous population of low-lying states of ions by electrons with the formation of hydrogen- and helium-like atoms can be responsible for the population of the split Stark levels in these atoms under the action of a Coulomb field. When electrons are captured during a collision by a "bare" nucleus inside a solid target, the Stark states of this atom will have the form of oscillations with period $2\pi\omega_s^{-1}$ ($\sim 10^{-15}$ sec). If in a thin target the ion period t_d is less than the period of the Stark-state oscillations, the ion at the exit from the target can retain the electrons in these low-lying states. Therefore, at the exit from thin carbon and gold targets (Tables III and IV) an anomalous population of argon states with charges 17^+ and 16^+ is observed.

When the ions are located in the target for a long time, i.e., $t_d \gg \omega_s^{-1}$, the relative significance of the substates in any subshell will be determined by a random distribution. Therefore, in thick targets no anomalous population of low-lying states is observed.

4. EQUILIBRIUM TARGET THICKNESSES AND CHARGE-STATE DISTRIBUTIONS FOR HEAVY IONS

For a detailed description of the charge states of heavy ions which have passed through thin layers of matter it is necessary to consider not only the mean charge, but also the real distribution of the charge states about the mean value, i.e., the relative intensities $F(q_i)$ of the various charge states which are present in the ion beam after it emerges from the target. The Bohr criterion determines only the mean value of the charge and does not give any information about other nearby charge states, especially when the values of q_i are far from $\bar{q}$.

The contributions $F(q_i)$ obtained for given q_i in various target materials can differ by many orders of magnitude. In principle, $F(q_i)$ can be calculated from the charge-exchange cross sections of the ion charge. However, as already noted, the charge-exchange cross sections are not known reliably enough, and there are no accurate data on their density dependence. Therefore, accurate theoretical calculations of $F(q_i)$ still cannot be carried out.

The equilibrium charge distributions of ions which have passed through various targets made of gases, vapors, and solids are shown in Fig. 8, taken from Ref. 9.

Aside from the differences between the average charges of ions which are formed in gases and in solid foils, it can be stated that even the distributions for the two types of target depend on the target type.

In the case of gaseous targets, the distributions produced in light targets (especially hydrogen) are considerably narrower and symmetrically shaped in comparison with the distributions obtained using heavier gases.

In solid targets the distributions are broader, as in heavy gases, and are more asymmetrically shaped. We note that for solid strippers the choice of target thickness strongly affects the values of the mean charge and the ion distribution in the charge.

In Fig. 9 we show the dependences of the yield of various charge states and the mean charge $\bar{q}$ of Cu^{9+} ions with energy 65 MeV on the thickness of the carbon target up to the equilibrium value.[38] Here for comparison we also show the calculated values of $\bar{q}$ obtained using Eq. (10) of Nikolaev and Dmitriev.[26]

The equilibrium target thickness increases somewhat for higher ion energies. As an example, in Fig. 10 we show the dependence of $\bar{q}$ on the energy of Kr ions and on the thickness of the carbon target.[31] It should be noted that, owing to multiple scattering, the use of a charge-exchange foil leads to an increase of the angular spread and to a slight smearing in energy of the energy loss. Therefore, it is necessary to choose the foil thickness with allowance for these factors.

Baron[39] approximated the equilibrium thicknesses of carbon foil by the simple analytic expression

$$x = 5.9 + 22.4\ E_p/A_p - 1.13\ (E_p/A_p)^2, \qquad (16)$$

TABLE IV. Fractions of charge states (%) of Ar (44 MeV/A) at the exit from a gold foil.

Thickness of the Au foil, $\mu g/cm^2$	Charge state of ^{40}Ar, %		
	16+	17+	18+
160	2	17	81
300	<0.5	10	90

TABLE V. Fractions of charge states of ^{40}Ar (44 MeV/A) after passing through Be and Au targets, normalized to 1.

Target	Thickness, mg/cm^2	Charge states of ^{40}Ar			
		18+	17+	16+	15+
Be	18.1	0.9997±0.0002	(3±1.5)·10^{-4}	(2±1)·10^{-6}	(7±4)·10^{-9}
	44.5	0.9996±0.0002	(3.5±2)·10^{-4}	(3±1.5)·10^{-6}	
	99	0.999±0.0006	(1.2±0.6)·10^{-3}	(2.5±1)·10^{-5}	
Au	39.9	0.85±0.03	0.14±0.03	10^{-2}	—
	96	0.89±0.03	0.11±0.03	—	—

where E_p/A_p is the particle energy, expressed in MeV/A, and x is expressed in μg/cm^2.

In Fig. 11 we show the charge distributions for uranium ions with energy 16.3 MeV/A after their passage through various materials.[34] We see that in this case equilibrium distributions with a higher value of the mean charge are obtained on carbon targets. Comparison of the distributions obtained after passage through gold and carbon charge-exchange targets shows that the center of the distribution from the carbon target is shifted by 9 units toward the charge state 78$^+$, while the intensity at the maximum is increased by an amount from 17 to 25%. To obtain equilibrium distributions at such energies for uranium it is necessary to use targets which are thicker ($\sim$500 μg/cm^2) than suggested by the estimates of Baron.[39]

We note that for heavy ions of a given energy the mean charge decreases and the width of the distribution increases with increasing atomic number of the charge-exchange target Z_t (Figs. 8 and 11).

As a rough approximation, the charge distributions can be approximated as Gaussian distributions:

$$F(q_i) = \frac{1}{\sqrt{2\pi}\, d} \exp\{-(q_i - \bar{q})^2/2d^2\}. \quad (17)$$

The width d of the distribution is defined as

$$d = \left[\sum_{q_i} (q_i - \bar{q})^2 F(q_i)\right]^{1/2}. \quad (18)$$

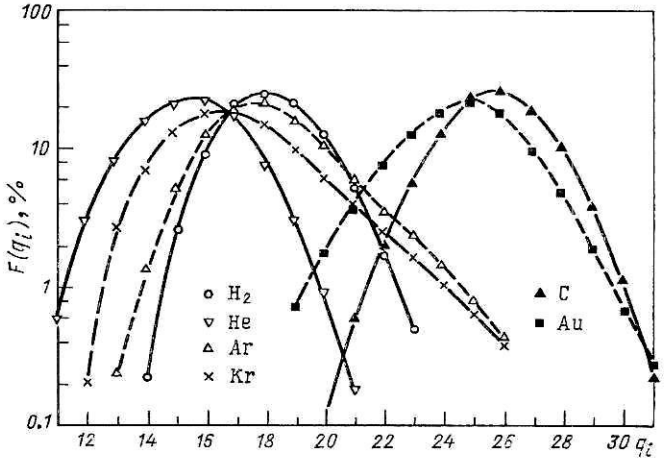

FIG. 8. Distribution of equilibrium charge states $F(q_i)$ for iodine ions of energy 110 MeV which have passed through various gaseous targets.

The distribution widths d are quite regular in a wide range of v_p and Z_p and can be approximated by semiempirical equations.

Dmitriev and Nikolaev[24] assumed that the width of the ion charge distributions are given by

$$d = d_1 Z_p^w, \quad (19)$$

where the parameters d_1 and w are determined empirically as functions of the mean ion charge. Their values are given in Table VI.

The accumulation of data on the charge distribution of heavy ions in air and in Formvar with energies up to 0.3 MeV/A and the subsequent analysis of Betz and Schmelzer[23] led to a different relation for the widths:

$$d = 0.27 Z_p^{0.5}. \quad (20)$$

These relations obviously do not take into account the dependence of d on the ion velocity, and therefore they are not useful approximations at higher energies. Nikolaev and Dmitriev[26] later obtained more realistic estimates of the dis-

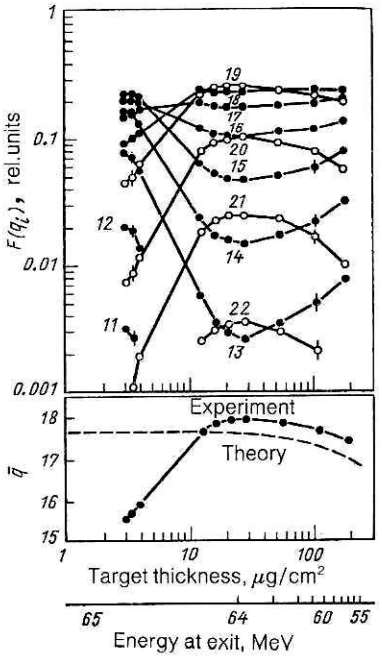

FIG. 9. Fractions of charge states $F(q_i)$ and mean values $\bar{q}$ obtained after passage through carbon foils of thickness from 3 to 183 μg/cm^2 for Cu^{9+} ions of initial energy 65 MeV (Ref. 38).

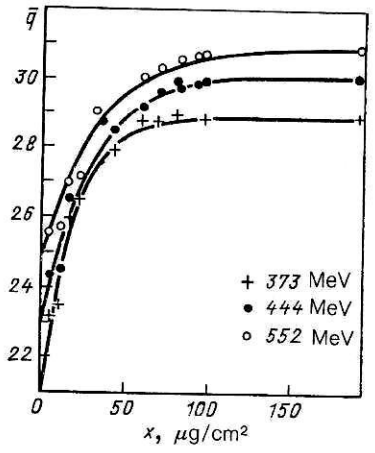

FIG. 10. Mean charge states of krypton ions for various energies as functions of the target thickness.

tribution widths after the passage of ions ($Z_p \geqslant 16$) through solid targets by introducing a dependence on $\bar{q}$ (or v_p):

$$d = d_2 \{\bar{q}[1 - (\bar{q}_0/Z_p^{1/K})]\}^{1/2}, \tag{21}$$

where $d_2 = 0.5$ and $K = 0.6$.

In many cases the maximum calculated widths deviate from the experimental values by less than 20%. Therefore, this relation is used most often to analyze the charge distributions.

It follows from Refs. 16 and 26 that the width of the distribution is a function of the "reduced" velocity X.

In Ref. 40 (for $Z_p \geqslant 8$) the values of d were approximated by the expression

$$d/Z_p^{0,4} = 0.426 - 0.0571X. \tag{22}$$

The comparison with the experimental data carried out by Ishihara *et al.*[16,41] showed that for ions of higher energy the widths of the distributions become narrow, owing to the absence of $q_i > Z_p$. In this case (for reduced velocities $X > 1$) d can be approximated by the expression

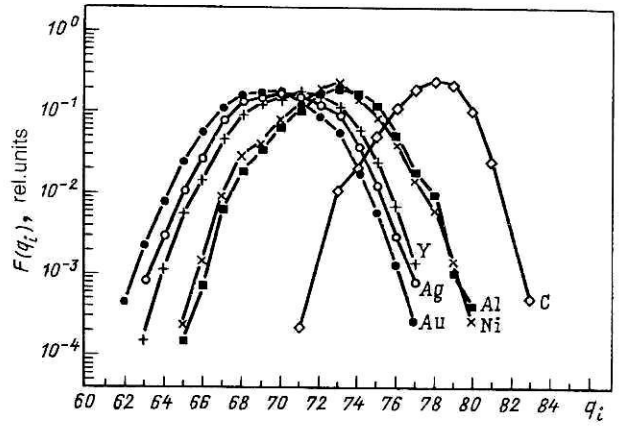

FIG. 11. Fractions of charge states $F(q_i)$ of uranium ions of energy 18.7 MeV/A after passing through various solid targets of thickness 500 μg/cm².

TABLE VI. The parameters d_1 and w in Eq. (19) describing the width of the charge distributions.

Medium	d_1	w
N_2, Ar	0.32	0.45
A solid	0.38	0.40

$$d/Z_p^{0,27} = 0.76 - 0.16X. \tag{23}$$

It should be noted that none of the approximations for d include the dependence on the target atomic number, even though $F(q_i) \sim f(Z_t)$, and therefore all the charge-state fractions $F(q_i)$ determined from $\bar{q}$ and d and calculated using a Gaussian distribution should be viewed as approximations. Moreover, for ions with small velocities and at higher energies the observed charge distributions differ significantly from the symmetric Gaussian distribution. The analysis carried out by Sayer[29] on the charge distributions of heavy ions of various energies at the exit from a carbon foil showed that asymmetric distributions of the charge states can be described by introducing the asymmetric function

$$F(q_i) = F_m \exp\{-0.5t^2/(1 + \epsilon t)\}, \tag{24}$$

where F_m is the fraction of charge with maximum intensity, $t = (q_i - q_0)/d$, q_0 is the charge of maximum strength, d is the width of the charge distribution, and ϵ is the asymmetry of the charge distribution (the skewness) with the small contribution $F(q_i)$, which was approximated as $\epsilon/d = A + BZ_p + Cd$.

In Refs. 40, 42, and 43 it was shown that the charge distributions of heavy ions as a function of the ion energy can be approximated by χ^2 functions and Gaussian and reduced χ^2 distributions. It was shown that the χ^2 distribution gives an excellent description of the distribution of heavy-ion charges at low ion velocities [$v_p < 2 \times 10^8$ cm/sec and $Z_p \leqslant 26$, and also for $0.4 \leqslant v_p$ (10^8 cm/sec) $\leqslant 1.2$, when $59 \leqslant Z_p \leqslant 82$].

At high velocities ($v_p > 3.6 \times 10^8 Z_p^{0.45}$ cm/sec and $7 \leqslant Z_p \leqslant 36$) the ion charge distribution is described by the reduced χ^2 function. The Gaussian distribution works well at intermediate energies (the range $23 \leqslant E_p/A_p \lesssim 1000$ keV/A). We note that the Gaussian distribution gives a good description of the distribution of heavy ions ($Z_p > 50$) beginning at $E_p/A_p > 5$ keV/A. The χ^2 and reduced χ^2 functions have a general expression for $F(q_i)$:.

$$F(q_i) = \left[2^{\frac{\nu}{2}} \Gamma\left(\frac{\nu}{2}\right)\right]^{-1} t^{\frac{\nu}{2}-1} \exp\left(-\frac{t}{2}\right), \tag{25}$$

where Γ is the gamma function, $c = 2(\bar{q} + 2)/d^2$, $\nu = 2(\bar{q} + 2)^2/d^2$, $t = c(q_i + 2)$ for the χ^2 distribution and $c = 2(Z_p - \bar{q} + 2)/d^2$, $\nu = 2(Z_p - \bar{q} + 2)^2/d^2$, $t = c(Z_p - q_i + 2)$ for the reduced χ^2 distribution.

The calculated and experimental values of $F(q_i)$ for Ar ions of various energies which have passed through carbon foil are compared in Fig. 12.

However, in a number of experimental studies it has been shown that the charge distributions deviate significantly from these theoretical distributions.[44–46] This is mainly

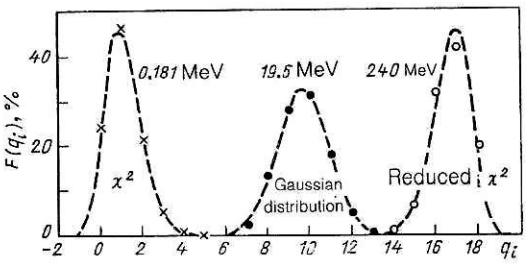

FIG. 12. Observed (points) and calculated (dashed lines) fractions of charge states of argon atoms of various energy at the exit from a carbon target. The calculations were carried out using the χ^2, Gaussian, and reduced χ^2 distributions in the study of Boudinet-Robinet (Ref. 43).

true of the distributions $F(q_i.)$ for $q_i. > \bar{q}$. Here in a number of cases it is clearly seen that the atomic shells of the heavy ion affect the equilibrium charge distributions of the heavy ions, leading to an increase or decrease of the fraction of particular charge states. As an example to illustrate such processes, we give the experimental results obtained by Moak *et al.*[44] for the charge distributions of Br ions of energy 100 and 140 MeV which have passed through carbon foil. From Fig. 13 we see that the fraction of charge states with $q_i > 25$ is decreased (when the M shell of the bromine atom contains no electrons).

5. THE INFLUENCE OF ATOMIC AND NUCLEAR EXCITED STATES IN HEAVY IONS ON THE ION CHARGE DISTRIBUTION

In Ref. 9 it was shown that for a wide range of velocities and types of accelerated heavy ions, the fraction of excited particles in the equilibrium beam after passing through a target is small, owing to the dominance of electron capture into the ground state of the ionized atoms. For heavy ions of relatively low energy, equilibrium between the electron capture and loss processes is reached after passage through several layers of the medium. The question boils down to whether or not these outer electrons are located in the ground state or in the residual excited shells of the ionized atom and can easily be ejected. Currently there are two models representations[47,48] of the interaction of a heavy ion with matter.

In the simplest interpretation based on the model of Bohr and Lindhard[47] it is assumed that collisions of ions with the atoms of a solid target lead to the excitation of the most weakly coupled electrons in heavy ions. Owing to rapid successive collisions, the excitation first acquired by one electron will be redistributed among a few of the closest electrons. Subsequent collisions increase the excitation of the weakly coupled electrons, leading to their loss. These resonance processes gradually build up on a certain number of electrons. As a result, a new equilibrium can be attained in which electron capture and loss are balanced, with the loss fraction increased owing to the decreased binding energy of the excited electrons. It should be noted that in this model most of the increase of the equilibrium charge occurs inside the matter. However, Bohr and Lindhard assumed that excitations of the residual electron shells of the ions in matter could lead to successive or cascade emission of electrons immediately after the ions exit into the vacuum, which can also increase the ion charge.

In a rarefied gas the time between two successive ion–atom collisions is considerably larger than in a solid, which makes it possible for the excitation energy acquired by the electrons in the first collision to be redistributed among several electrons and their excitation to be removed. In this case the effective cross sections for electron loss are decreased, as a result of which the mean charge of the ion does not increase greatly in the passage of the ion through a gaseous medium.

Without making any special distinction for gases, in their model Betz and Grodzins[48] assume that when an ion passes through the target material its charge states differ greatly inside and outside the target. Owing to multiple collisions, an electron shell of the ion is fairly strongly excited, so that there is a high probability for the ion as it exits from the target to remove its excitation by one or several Auger cascades. Therefore, according to this model the charge states of a heavy ion in a target are lower than those measured for the same ion some time after it has left the target (Fig. 14).

The experiments of Della-Negra *et al.*[49] showed that for heavy ions up to Ar there is a small difference between the mean value of the charge in gases and solids at ion energies of about 1 MeV/A. Also, in this energy range there was not found to be any difference in the mean charge states of the ions at the exit from the target and at some distance from the target. Multiple excitation becomes more important for hea-

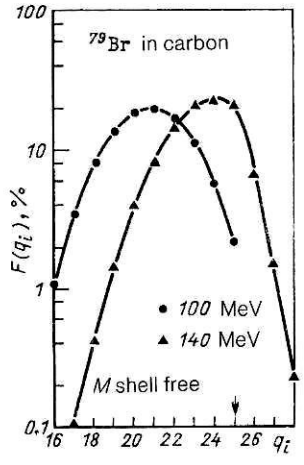

FIG. 13. Distribution of charge states of bromine ions of various energies at the exit from a carbon foil.

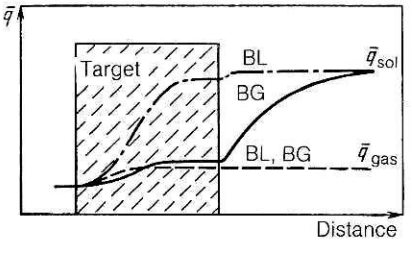

FIG. 14. Schematic illustration of the change of the mean charge of a heavy ion passing through gaseous and solid targets. The hatched region represents the target. BL refers to the Bohr–Lindhard theory, and BG refers to the modified Betz–Grodzins theory.

vier ions. The ions crossing the exit surface of the target have higher excited states of the atomic electrons than at the entrance to the target. For example, for krypton ions of energy 1.16 MeV/A the authors found that the mean charge states of these ions at the exit from the target are 1.6–3 charge units lower than those measured later in a vacuum (70 nsec after emission from the target). This increase is a consequence of the subsequent decay of the excited states (autoionization) with the emission of Auger electrons. On the basis of these and other experiments carried out recently there is no reason to give preference to any particular one of the models discussed above, even though the authors of Ref. 49 view their results as proof of the model of Betz and Grodzins.

We add that both models assume that equilibrium is reached rapidly, owing to ionization of the outer shells and electron capture, so that a balance has been reached after a few layers of the target material have been traversed. This assumption is not fully valid in collisions of heavy ions with heavy atoms and, in particular, symmetric systems, when collisions with atoms lead to the ionization of inner shells.

Study of the charge distributions of heavy ions (especially scattered ions) produced by various targets has shown that the high-charge fraction is present with a probability considerably higher than expected from calculations. The presence of such highly charged ions has been attributed to the ionization of an inner shell in collisions with small impact parameter and with the creation of one or more vacancies.[10,50]

In Ref. 51 it was shown that the filling of a vacancy in an inner atomic shell can lead to cascade ionization with the number of electrons depending on the shell in which the vacancy was created and on the atomic number Z of the atom.

In collisions of heavy ions (Pb + Pb, U + U, etc.) at small impact parameters it is expected that K- and L-shell ionization can reach 10^{-1} (Ref. 52) per interaction.

Since the lifetimes of ionized states in heavy atoms in the K- and L-shells reach 10^{-15}–10^{-17} sec (Refs. 52–54), it can be hoped that some of the excited ion states survive after emission from the target. This would make it possible to have effects leading to autoionization or cascade ionization of the atoms, which would be significant for relatively thin targets (when the time for the ion to pass through the target is small). In fact, it has been found that in near collisions of heavy ions the charge distributions become asymmetric or are shifted to higher charge states. Stiebing and coworkers[52,55] have studied the ion charge distributions of products of the scattering of ^{208}Pb (5.9 MeV/A) on gold targets of various thicknesses at angles of from 5 to 35°. Both ^{208}Pb and ^{197}Au ionized atoms were detected.

For thin targets (up to 100 μg/cm^2) a shift of $\bar{q}$ due to ionization of inner shells has been observed (Fig. 15). These effects appear most clearly for targets of thickness 20 μg/cm^2.

For thicker targets (370–870 μg/cm^2) a clear asymmetry in the distribution is observed ($\sim$10% over 10 units of charge). Such distributions can only arise from the fact that for thin targets many vacancies in the inner shells of ionized ^{208}Pb atoms survive until emission from the target. Their subsequent decay leads to the cascade ionization of isolated atoms which have been emitted.

Measurements of the charge distributions of ^{208}Pb ions scattered at an angle of 5° have not revealed any noticeable anomalies, which indicates that near collisions give a small contribution.

We note that the measured charge distributions of ^{197}Au ions knocked out into forward angles (35°) (Ref. 55) have a form (Fig. 16) similar to that of the ^{208}Pb distributions (Fig. 15).

The detection of elastically scattered interaction products of the complex system Pb + Au at the angle 35° corresponded to an impact parameter of 6–10 F, which, in the opinion of the authors,[52] is fully capable of leading to the creation of a quasimolecular system with excitation of the inner atomic shells.

For nuclear reactions involving heavy ions ($A\sim$20–40), estimates indicate that in the Coulomb interaction with nuclei of intermediate and large mass numbers the K-shell ionization can reach 10^{-3}–10^{-4} (Ref. 53) per nuclear reaction, and, owing to shakedown, the M-shell ionization can reach $\sim 10^{-2}$ (Ref. 54). It would therefore seem that the ionization of nuclear-reaction products need not manifest any special anomalies if the effect of nuclear processes on the ionization of the recoil atoms is neglected. In fact, excited nuclear states strongly affect the ionization of inner atomic shells, owing to conversion of nuclear transitions of the nuclear-reaction products.[57–63] The vacancies formed in con-

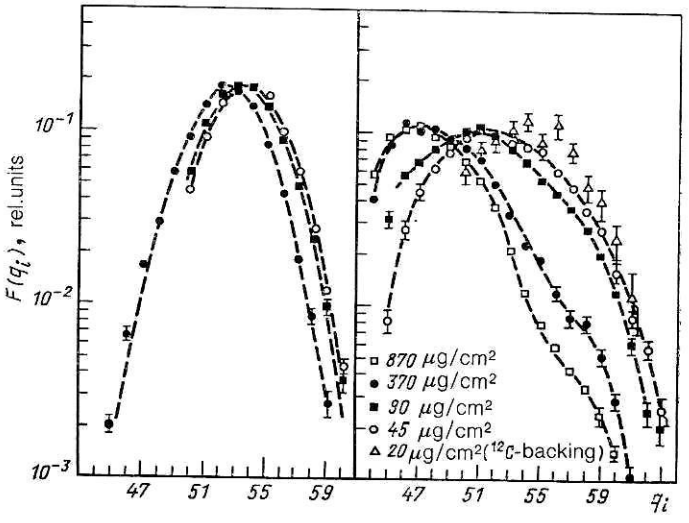

FIG. 15. Distribution of charge states of heavy lead ions of energy 5.9 MeV/A scattered on gold targets of various thicknesses at angles of 5° (left-hand side) and 35° (right-hand side).

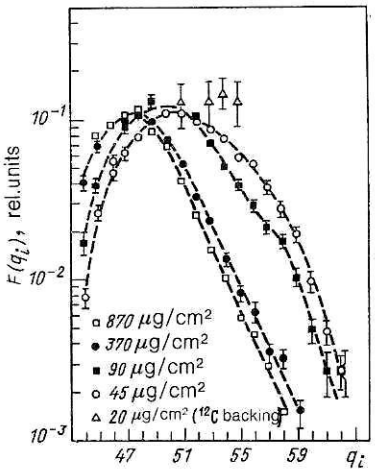

FIG. 16. Charge distributions of ^{197}Au recoil nuclei scattered at an angle of 35° from targets of various thicknesses in the bombardment of ^{197}Au by heavy ^{208}Pb ions of energy 5.9 MeV/A.

version on inner shells of ionized atoms (reaction products) lead to Auger cascades, which significantly increase the ion charge states over the expected equilibrium values.

Wieclawick[56] first observed highly charged states of ^{237}Np recoil atoms after the α decay of ^{241}Am. In addition to the fundamental singly charged ^{237}Np recoil atoms, various charge states up to 20^+ were observed.

Later it was shown that the products of nuclear reactions involving heavy ions in a wide range of atomic numbers[57–66] have asymmetric charge distributions shifted to higher values of the charge relative to the equilibrium distributions.

This shift of the charge distributions of reaction products was first observed for rare-earth elements, in particular, isotopes of Dy, and also isotopes of Po (Refs. 57–62).

In Fig. 17 we show the charge distributions of ionized recoil atoms ^{147}Dy produced in the nuclear reaction ^{114}Cd(^{40}Ar, $7n$)^{147}Dy, and also of recoil atoms ^{199}Po produced in the reaction ^{164}Dy(^{40}Ar, $5n$)^{199}Po.

The data are presented in the form of the dependence of the percentage contribution of the intensity of a given charge state $F(q_i)$ to the total charge distribution $\Sigma F(q_i)$ on the distance along the focal plane of the magnetic analyzer (x) or the ion charge (q_i).

The experimental contributions of each charge state as a function of the degree of ionization of the recoil atoms knocked out of the target are shown as a histogram. The solid line shows the charge distributions of the recoil atoms after passing through a thin carbon foil, and the arrows indicate the values of the mean charge calculated using Eq. (10) of Nikolaev and Dmitriev.[26]

Analysis of the possible ionization mechanisms has shown that the dominant one leading to additional ionization of isolated atoms moving in a vacuum is the ionization of inner shells owing to γ conversion in nuclear cascades. Owing to the large number of transitions with γ emission, in reactions with heavy ions there is a large probability for producing several vacancies in low-lying atomic shells.[57,61]

The dashed lines show the separate contributions of various ionization mechanisms to the experimental distribution. The lines labeled n show the part corresponding to the initial ionization with width of the distribution d determined from (21). The contribution of the first ionization to the total distribution in the range of recoil atoms under consideration is small and lies in the range from 10 to 30%. It is obvious that in the nuclear mass range $A > 147$ from 70 to 90% of the recoil atoms produced undergo autoionization (or second ionization) owing to the ionization of the K, L, and other atomic shells via the internal conversion of several nuclear transitions.

The dashed lines 1, 2, 3, ... show the contributions of the successive conversion events leading to autoionization of the recoil atoms and to an increase of the mean charge. The number and magnitude of these contributions can be used to estimate the number of converted nuclear transitions and the degree of their conversion. Extension of the region of investigation of ionized products of nuclear reactions involving heavy ions has shown that for relatively small atomic numbers ($Z_p \sim 20$–30) the charge distributions of the ionized reaction products[61,62] are close to the values predicted[26,32] assuming ordinary equilibrium ionization based on (10), (13), and (15). This is apparently related to the low probability for internal conversion of excited states of nuclear products in this range of mass numbers. The fission fragments and recoil atoms (with $Z_p \simeq 50$) produced in nuclear reactions involving heavy ions[63–65] have values of the charge $\bar{q}$ higher than predicted. Here for recoil atoms of tin the isotopic dependence on the time of travel of the ionized atoms in the vacuum, observed in the recoil-atom charge distribution, indicates that among these nuclides there are various isomer states[66,67] with lifetimes in the nanosecond range (Fig. 18).

As Z_p and the excitation energy of the created product nucleus increase, both the density of the excited states and the probability of internal conversion grow.

Broad ion charge distributions have been observed for products of (α, xn) nuclear reactions in the region of the

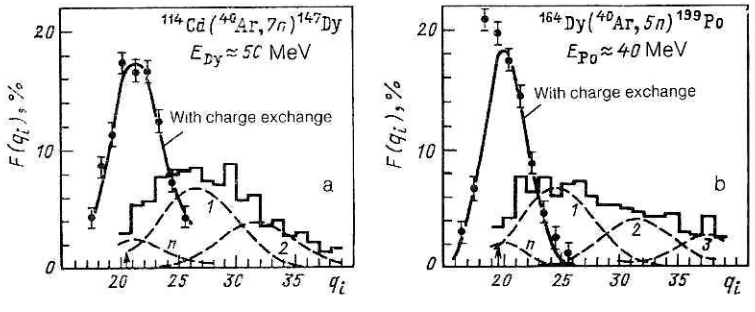

FIG. 17. Charge distributions of the reaction products ^{147}Dy and ^{199}Po knocked out of ^{114}Cd (a) and ^{164}Dy (b) targets, respectively. The histograms show the charge distributions of ^{147}Dy and ^{199}Po atoms knocked out directly from the target. The solid lines with the points correspond to the distributions of these atoms after passing through an additional carbon foil of thickness 50 μg/cm², and the arrows indicate the expected values of the mean charge (Ref. 26).

transuranium elements. This is due to the development of Auger cascades in isomer or rotational transitions in the produced nuclei.[68]

For the products of nuclear reactions involving heavy ions produced in this mass range, it can be expected that the charge distributions are broader than for Pb or Po (Refs. 60 and 61) and that the mean charge is higher. Here it should be noted that all the charge distributions of the product ions will naturally be strongly asymmetric and cannot be described by any of the distributions discussed above.

By using an additional thin foil (a plunger) behind the target at various distances from the target, it is possible to make rough estimates of the lifetimes of such converted isomer states[66–68]

As was shown in Refs. 58 and 69–71, the use of additional foil plungers with thicknesses close to the equilibrium value and located at a certain distance from the target significantly raises the efficiency of collecting heavy reaction products. The ionization of heavy ions and, particularly, of the products of nuclear reactions involving heavy ions obviously requires further study and systematization in a wider range of Z_p and recoil energy.

6. EFFECT OF THE PROPERTIES OF A SOLID TARGET ON ATOMIC COLLISIONS INVOLVING HEAVY IONS AND PROCESSES ACCOMPANYING ION PASSAGE THROUGH THE TARGET

The study of the effects of the properties of a solid material on ion–atom collisions is a very complicated problem. For solid targets it is necessary at least to take into account the effect of the valence electrons (conduction electrons), the orientation of the periodic lattice, and surface effects. It should be noted that the valence electrons in solids have a zonal structure and lead to the appearance of collective oscillations. Many physical phenomena arise in atomic collisions with a very limited surface of the solid. For example, at a distance of about 0.01 nm from the surface of a metal the electron density vanishes. Both the lattice constant and the lattice vibrations in a solid undergo a change in the regions closest to the surface. The zonal structure and collective motion of the valence electrons near the surface also differ from their form inside the target.

Recently there has been considerable progress in the description of ion–atom interactions, owing to the increased interest in applications to many fields of study, such as thermonuclear fusion (the plasma–wall interaction), surface-structure analysis, ion implantation, and so on. In an interaction with a solid, most of the energy is consumed by electron excitations of $\sim 10^4$ eV over 1 nm. This huge energy density and the overlap of complex cascades at ion-induced defects lead to characteristic features such as the formation of tracks visible with an electron microscope, apparently caused by the destruction of the atomic planes. For example, a single fission event in a crystal creates about 10^5 displaced atoms.[4]

Let us consider a few of the possible mechanisms for electron excitation in a solid, primarily, the excitation of inner-shell electrons in atomic collisions. The inelasticity resulting from electron excitation begins to manifest itself when the L shells overlap by the maximum amount.

The next stage, associated with the absorption of a large energy, occurs when the K shells overlap. The excitation energy reaches 10^3 eV. Nevertheless, for heavy ions of energy above 1 MeV/A, the fraction of kinetic energy lost in such collisions becomes relatively small. Moreover, the shells can overlap sufficiently strongly only for nearly head-on collisions, but such collisions are rare. Nuclear collisions occur even more rarely.

The excitations of valence electrons is by far the most probable. When a heavy ion of velocity v_p passes near an electron located in an energy level with ionization energy E_i, when their short-lived collision occurs the Coulomb field is

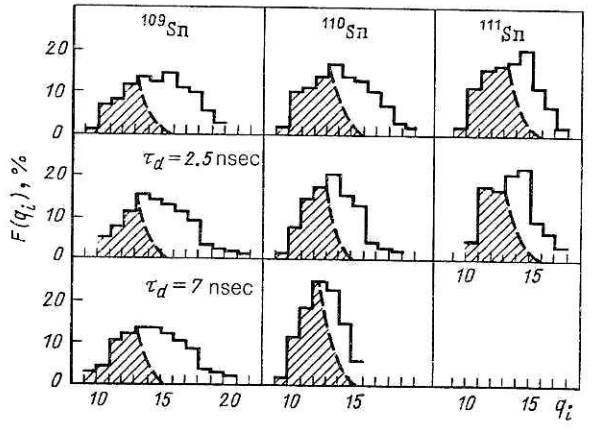

FIG. 18. Charge distributions of products of the reaction $^{26}Ne + Zr \rightarrow {}^{109}Sn$, ^{110}Sn, and ^{111}Sn (with $E_{Ne} \simeq 14$ MeV) immediately after passing through a Zr target (top row), after a plunger in the form of carbon foil located a distance from the target corresponding to a reaction-product travel time of 2.5 nsec (middle row), and after a plunger located at 7 nsec (bottom row). The dashed line shows the calculated ionization.

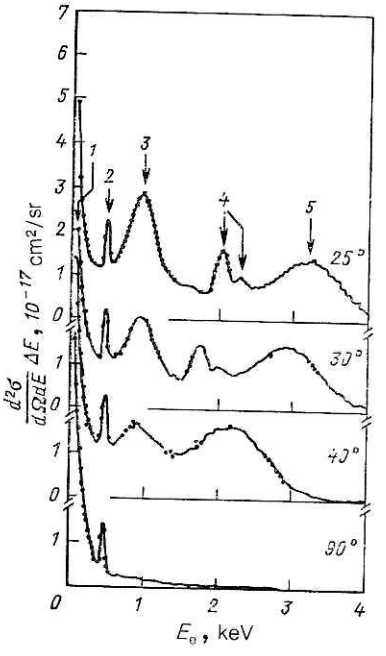

FIG. 19. Differential cross sections for electron emission in collisions of oxygen ions (O^{5+}) of energy 30 MeV with oxygen molecules, measured at various emission angles. The following structure can be identified: 1—electrons emitted from the target in "soft" collisions; 2—Auger electrons from the target; 3—elastically scattered electrons from the incident heavy ion; 4—Auger electrons from the incident ion; 5—electrons from the target in "binary" collisions.

perturbed for a time $\sim a_0/v_p$ (a_0 is the Bohr radius). This perturbation leads to ionization of the atom and to the emission of secondary electrons. The measured secondary-electron spectra reveal a distinct structure which can be attributed to individual processes of electron excitation and de-excitation in the target atoms or the incident ions.

In Fig. 19 we show the experimental results for the cross sections for electron production in the passage of oxygen ions of energy 30 MeV through oxygen[72] [the system O^{5+} (30 MeV) + O_2]. The spectral structure is expressed most clearly at forward electron emission angles. For this system it was found that electrons emitted from outer shells of the heavy ion dominate at small angles. Auger electrons emitted from the incident heavy ion are observed at angles below 40°, and their yield depends on the ion charge state (Fig. 20). Auger electrons from the target are observed at all angles.

Elastically scattered electrons from the incident ion are most intense at forward angles and when the charge of the heavy ion is small. We note that two contributions dominate in the electron continuum spectrum. The electrons produced in "soft" and "binary" collisions (with the minimum and maximum momentum transfer from the incident ion to the target atom, respectively) behave differently. The electron spectra in soft collisions are practically isotropic in intensity and the peak position, whereas in binary collisions the maximum yield shifts dramatically to lower energies with increasing angle and vanishes at emission angles larger than 90° (Fig. 19).

The binary peak can be described theoretically as classical two-body collisions of quasifree target electrons scattered on the projectile nuclei. As far as the spectrum of the so-called soft collisions is concerned, owing to the large impact parameter in the interaction of the projectile electrons with the target electrons the electron emission can be viewed as a two-center electron-emission process. In the case of fast highly charged ions the strength of the scattering potential is increased relative to that for light ions, and this process must become dominant in δ-electron emission.

Studies of δ-electron emission in collisions of highly charged heavy ions U^{33+} (1.4 MeV/A) with Ar (or Ne) (Ref. 73) indicate that there is no clearly noticeable structure, and the dominant contribution to the continuous spectrum comes from the δ electrons of the soft spectrum, which falls off exponentially with the electron energy (Fig. 21).

In contrast to the case of light ions interacting with a gas, at higher energies of the δ electrons emitted in binary collisions a strong anisotropy relative to the scattering trajectory appears and there is a sharp peak at 60° with energy 2250 eV, while at angles of 90° and higher no δ electrons are observed at all. The strong repulsive Coulomb field of the projectile induces a large polarization of the target shells and emission of collective electrons in the scattering plane in the direction opposite to the target-atom recoil.

The two-center ionization mechanism can be represented as an acceleration of electrons from a bound state to the continuum. The field of a rapidly moving projectile focuses several accelerated electrons in a small angular cone at $\theta \simeq 60°$, with all the electrons having similar energies ($\Delta E \sim 300$ eV).

A sharp increase in the emission of δ electrons and high-energy positrons is observed in collisions with very heavy ions. For example, for the system U + Pb (14.7 MeV/A) δ electrons have been detected with kinetic energy up to 2.4 MeV, which is 20 times higher than the binding energy of K electrons in uranium atoms. This high-energy electron component can be attributed to the emission of strongly bound electrons produced in the interaction of quasiatoms with the combined charge.[74]

When heavy ions interact with atoms, in addition to atomic-level excitation another possible mechanism is that

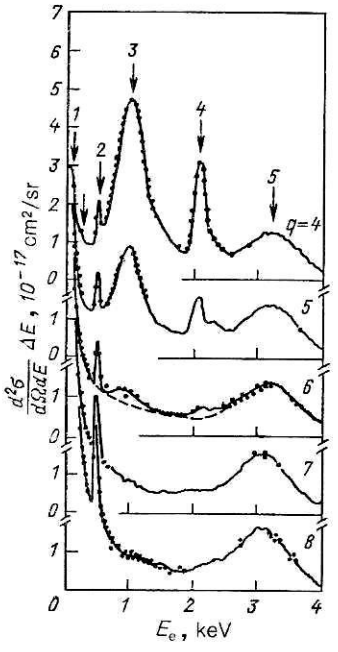

FIG. 20. The same dependences as in Fig. 19 at an emission angle of 25° from the charge state q of oxygen ions.

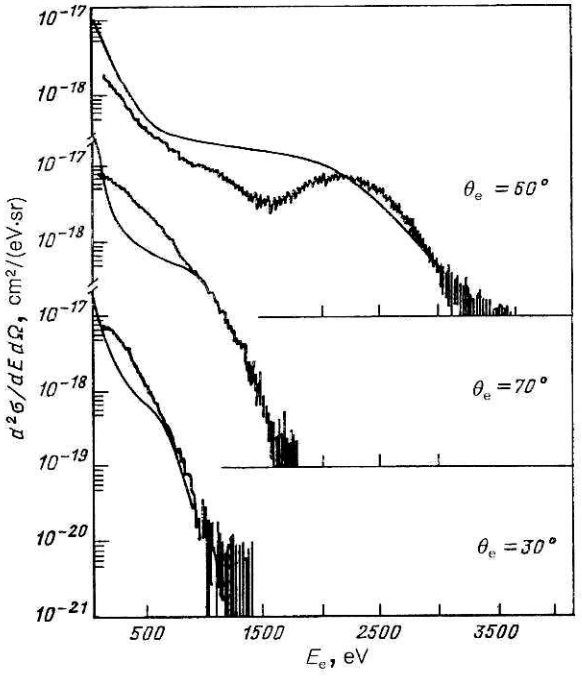

FIG. 21. Differential cross sections for electron emission in the energy range from 200 to 4000 eV in collisions of U^{33+} at 1.4 MeV/A with Ar at various emission angles.

of the emission of photons with a continuous radiation spectrum, owing to three types of source: radiative electron capture, transitions between molecular orbitals, and the distinct bremsstrahlung of charged particles and secondary electrons. Not all of these processes have been sufficiently well studied.

The phenomenon of radiative electron capture (REC) is described in Ref. 75.

Radiative electron capture corresponds to a process in which a moving heavy ion captures a free or weakly bound target electron and emits a photon whose energy is determined by the binding energy and kinetic energy of the electron relative to the moving ion and is independent of the target material. The photon angular distribution is proportional to $\sin^2\theta$ (where θ is the angle between the directions of the moving ion and the emitted photon). The REC-radiation peak is observed most clearly when $v_p \gg v_e$, where v_e is the velocity of the captured electron.

The structure of the REC characterizes the ion charge distributions, since it is reflected in the binding energy of the captured electron. For small particle velocities ($v_p \leqslant v_e$) an ion and an atom of the medium can combine to form a quasimolecule. Electron transitions between quasimolecular states also lead to the creation of molecular-orbital radiation spectra (MO radiation).[76,77]

The strength of this radiation falls off exponentially with increasing photon energy. When the colliding nuclei are heavy, the observed spectrum has a more complicated structure, owing to electron transitions into the deeper orbitals formed in the quasimolecule during these collisions.

Owing to the presence of electrons with $v_e > v_p$ and $v_e < v_p$, both REC and MO radiation are usually observed in experiments. When heavy ions pass through matter, electron capture and loss processes lead, as mentioned above, to a multiple change of the ion charge and, accordingly, of the current density. A consequence of this must be the appearance of electromagnetic radiation,[78] the properties of which must be determined by ion charge-exchange processes in the medium. Attempts to find this radiation experimentally have not yet been very successful.

CONCLUSIONS

It is clear from our discussion that there are many problems in the study of ion–atom collisions in various media. New theoretical approaches and new experiments will be necessary to solve these problems. As we noted above, the following problems remain in the study of the charge distributions of heavy ions and ionized reaction products.

1. There is no quantitative description of charge-exchange processes in the passage of heavy ions through various media, including density effects and the charge distributions of the particles in the matter and at the exit from the target.

2. Further study is needed of the anomaly in the heavy-ion distribution, in particular, the behavior of the widths of the ion charge distribution and the equilibrium charges. This is particularly true for ions heavier than Xe, where the observed mean charges are smaller than the predicted values.

3. Study of the charge exchange of heavy ions in a medium at intermediate energies (20–50 MeV/A) has led to the observation that there is a high probability for forming hydrogen- and helium-like atoms at the exit from thin targets (up to 150–200 μg/cm^2). Here the stripping on lighter targets is worse than observed for heavy ions at energies of up to 10 MeV/A.

4. Further study is needed of the behavior of the mean and equilibrium charges of products of nuclear reactions involving heavy ions in various media in a wide range of atomic numbers, particularly for transuranium elements.

5. More attention should be paid to the problems in studying the processes accompanying the passage of heavy ions through matter, and the structural changes in the target material resulting from the passage of ions of various charge.

APPENDIX. ENERGY LOSSES AND THE EFFECTIVE CHARGE OF THE PARTICLES

For heavy ions passing through matter, the energy losses are mainly due to discrete random collisions. The statistical nature of the ionization and excitation processes of both the target atoms and the projectile atoms leads to fluctuations in the ion energy loss (straggling).[79,80]

Aside from its fundamental importance for atomic collision processes, knowledge of energy-loss straggling is important for most accelerator-based experiments.[39] Energy-loss straggling imposes limits on the Z-resolution of ΔE detectors and on the degree of splitting of the ion beam. Processes of ion-charge variation in gases, i.e., fluctuations of the charge states, give the dominant contribution to straggling. The main contribution to the ion energy losses comes from long-range interactions, while near collisions with atoms of the medium affect the straggling.

Let us consider the relation between the mean equilibrium charge determined from the heavy-ion ionization and the effective charge determined from the energy losses. The electron bremsstrahlung cross section of heavy ions in a medium S_e (henceforth this will simply be called S) is closely related to the ion charge states.

In the Bethe–Bloch energy range the bremsstrahlung cross section is proportional to the square of the effective charge (q_{ef}) of the ion:

$$S = q_{ef}^2 f, \tag{26}$$

where f is a function of the ion energy and the mean ionization potential, corrected for the dependence on Z_p and Z_t of the medium. Assuming that the functions f are the same for light particles (LI) and for heavy ions (HI) at the same velocity in a given medium, the effective charge of the heavy ions can be defined as

$$(q_{ef})_{HI} = (q_{ef})_{LI}\,(S_{HI}/S_{LI})^{1/2}. \tag{27}$$

Comparison is usually made with a light ion—a proton.[81] In this case

$$S_{HI} = (q_{ef})^2\, S_p, \tag{28}$$

where S_{HI} and S_p are the bremsstrahlung cross sections of heavy ions and protons at the same velocity and in the same medium.

As was first shown by Bohr, the effective charge is characterized by the average charge during its deceleration process. Assuming that q_{ef} is equal to the rms equilibrium charge $\bar{q}$, as a first approximation for gases we can assume

that $q_{ef} = Z_p^{1/3} v_p / v_0$ and is independent of Z_t of the medium.

The later calculations of Ziegler[83] with a slight change of the Bohr criterion define q_{ef} as

$$q_{ef} = Z_p \{1 - \exp(v_2)\,[1.034 - 0.177 \exp(-0.08114\, Z_p)]\},$$

where $v_2 = v_1 + 0.0378 \sin(0.5 v_1 \pi)$, $v_1 = 0.886 (v_p/v_0) \times Z_p^{-2/3}$, v_0 is the Bohr velocity.

However, the accuracy of these calculations is limited by the lack of dependence of q_{ef} on Z_t of the braking medium. The good agreement obtained between the measured values of $\bar{q}$ and the calculated q_{ef} in light gases[47,48] was later taken as physical justification for Eq. (28). In fact, for heavy ions the behavior of $\bar{q}$ and q_{ef} is similar,[80,81] just as for $\bar{q}$:

1) q_{ef} increases smoothly in passage through lighter braking media (with decreasing Z_t), and this dependence is manifested more sharply with increasing energy;

2) at energies close to 1 MeV/A and in other energy ranges q_{ef} has a pronounced oscillatory dependence on Z_t (Fig. 22).

The experimentally observed oscillation phases of S_{HI} appear in the same locations as in the case of α-particle bremsstrahlung, with the maxima near $Z_t \simeq 20$, 40, and 60, and are characterized by the structure of the atomic shells of the medium. However, the oscillation phases for $\bar{q}$ and S_{HI} as functions of Z_t are different. Whereas the oscillation phases of S_{HI} are almost independent of E_p and Z_p (Refs. 80 and 82), for $\bar{q}$ they vary with E_p and Z_p, with the maxima of the oscillations in $\bar{q}$ (Ref. 6) corresponding to the maximum of the capture cross sections (σ_c). To estimate the latter it is necessary to take into account the vacancies in the electron shells of the ion (Fig. 23).

In Fig. 22 we show the experimental values of q_{ef} for ions of U, Pb, W, Xe, and Kr with energy 0.6 MeV/A in various solid targets. The systematic Z_t dependence of q_{ef} (10–20%) is clearly seen. This mainly reflects the difference in the Z_t oscillations from case of protons at the same velocity.

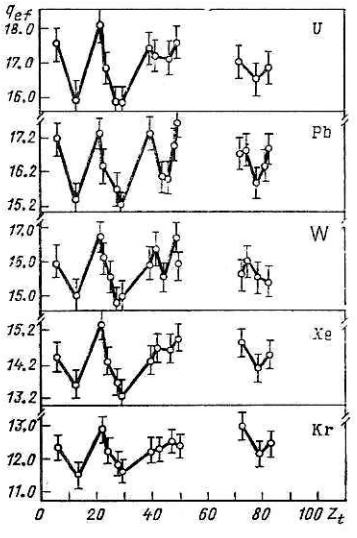

FIG. 22. Values of q_{ef} for various heavy ions of energy 0.6 MeV/A as a function of Z_t of the medium.

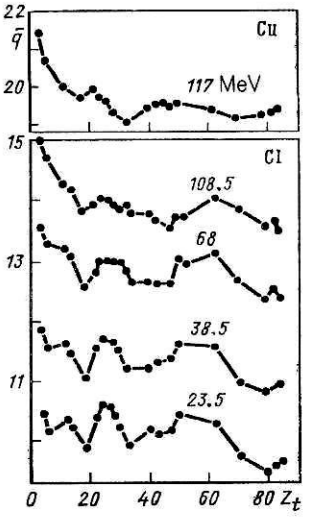

FIG. 23. Mean equilibrium values $\bar{q}$ for heavy ions of Cu(117 MeV) and Cl from 23.5 to 108.5 MeV after passing through various solid targets.

The values of q_{ef} in gases are also lower than in solid targets. The difference of q in gas and solid targets becomes more obvious with increasing ion energy,[81] when the Z_t oscillations in S_{HI} are somewhat smeared out, except for very light targets. This makes it necessary to revise the theoretical approaches and to take into account the Z_t oscillations in q_{ef}.

In Fig. 24 we compare the experimental values of q_{ef} and $\bar{q}$ for Kr, Xe, Pb, and U ions of energy 1.4 MeV/A in argon.[81] We see from this figure that these quantitites coincide for relatively light ions up to Kr, while for heavier ions $\bar{q}$ is larger than q_{ef}. For ions of lead and uranium this difference reaches 15%.

If q_{ef} is interpreted as the average value of the charge inside the target, the difference between q_{ef} and $\bar{q}$ should be related to the emission of Auger electrons of residual excitations of atoms leaving the target.

However, as was pointed out in Ref. 82, the meaning of the effective ion charge is not completely clear. The point is that in calculations of the dependence of the ion bremsstrahlung cross section on $q_{ef} \sim f(Z_p)$ at low energies, higher-order terms of the Z_p dependence are neglected in the approximation functions, which means that q_{ef} cannot be identified with the mean charge inside the target.

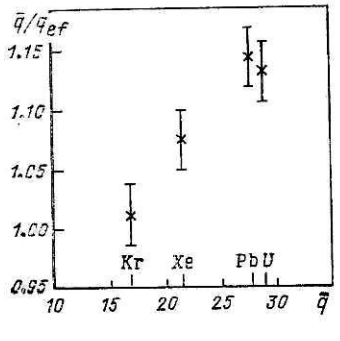

FIG. 24. Comparison of the values of $\bar{q}/q_{ef}$ and $\bar{q}$ for various heavy ions (Kr, Xe, Pb, and U) of energy 1.4 MeV/A in passing through argon.

At intermediate energies (for example, 25 MeV/A for Ar) agreement can be obtained in the bremsstrahlung cross sections[82] by assuming that the effective charge is several percent smaller than the mean charge $\bar{q}$ determined from the ionization. Given these uncertainties, the difference between q_{ef} and $\bar{q}$ cannot be quantitatively related to the number of emitted Auger electrons.

[1)]The term "heavy ions" usually refers to ions with atomic number larger than that of helium ($Z_p > 2$).

[1]H. S. W. Massey and E. H. S. Burhop, *Electronic and Ionic Impact Phenomena* (Clarendon Press, Oxford, 1952) [Russ. transl., IIL, Moscow, 1958].
[2]N. F. Mott and H. S. W. Massey, *The Theory of Atomic Collisions*, 3rd ed. (Clarendon Press, Oxford, 1965) [Russ. transl., Mir, Moscow, 1969].
[3]I. A. Akhiezer and L. N. Davydov, *Introduction to the Theoretical Radiation Physics of Metals and Alloys* [in Russian] (Naukova Dumka, Kiev, 1985).
[4]Y.-H. Ohtsuki, *Charged Beam Interaction with Solids* (Taylor and Francis, New York, 1983) [Russ. transl., Mir, Moscow, 1985].
[5]A. B. Wittkower and H.-D. Betz, At. Data **5**, 113 (1973).
[6]K. Shima, T. Mikumo, and H. Tawara, At. Data Nucl. Data Tables **34**, 357 (1986).
[7]V. S. Nikolaev, Usp. Fiz. Nauk **85**, 679 (1965) [Sov. Phys. Usp. **8**, 269 (1965)].
[8]V. S. Nikolaev, Zh. Eksp. Teor. Fiz. **51**, 1263 (1966) [Sov. Phys. JETP **24**, 847 (1967)].
[9]H.-D. Betz, Rev. Mod. Phys. **44**, 465 (1972).
[10]B. Delaunay, Nucl. Instrum. Methods **146**, 101 (1977).
[11]N. Bohr, Phys. Rev. **58**, 654 (1940); **59**, 270 (1941).
[12]W. E. Lamb, Phys. Rev. **58**, 696 (1940).
[13]N. O. Lassen, Phys. Rev. **79**, 1016 (1950).
[14]R. B. Clark, I. S. Grant, R. King *et al.*, Nucl. Instrum. Methods **133**, 17 (1976).
[15]V. Z. Maĭdikov, Yu. V. Gofman, G. S. Popeko, and N. K. Skobelev, Prib. Tekh. Eksp. No. 4, 68 (1979).
[16]T. Ishihara, K. Shima, T. Kimura, *et al.*, Nucl. Instrum. Methods **204**, 235 (1982).
[17]L. A. Petrov, V. A. Karnaukhov, and D. D. Bogdanov, Zh. Eksp. Teor. Fiz. **59**, 1926 (1970) [Sov. Phys. JETP **32**, 1042 (1971)].
[18]A. Ghiorso, M. Leino, S. Yashita, P. Armbruster, *et al.*, Scientific Report GSI 83-1 (1982), p. 70; A. Ghiorso, S. Yashita, M. E. Leino, *et al.*, Nucl. Instrum. Methods **A269**, 192 (1988).
[19]G. Ryding, A. B. Wittkower, and P. H. Rose, Phys. Rev. **185**, 129 (1969).
[20]N. Bohr, K. Dan. Vidensk. Selsk. Mat.-Fys. Medd. **18**, No. 8 (1948).
[21]G. I. Bell, Phys. Rev. **90**, 545 (1953).
[22]J H. Brunings and J. K. Knipp, Phys. Rev. **59**, 919 (1941).
[23]H.-D. Betz and Ch. Schmelzer, Unilac Report 1–67, Heidelberg University (1967).
[24]I. S. Dmitriev and V. S. Nikolaev, Zh. Eksp. Teor. Fiz. **47**, 615 (1964) [Sov. Phys. JETP **20**, 409 (1965)].
[25]H.-D. Betz, Y. Hortig, E. Leischner, *et al.*, Phys. Lett. **22**, 643 (1966).
[26]V. S. Nikolaev and I. S. Dmitriev, Phys. Lett. **28A**, 277 (1968).
[27]K. X. To and R. Drouin, Phys. Scr. **14**, 277 (1976); Nucl. Instrum. Methods **160**, 461 (1979).
[28]E. Baron, J. Phys. (Paris) Colloq. CI Suppl. 40, Cl (1979).
[29]O. Sayer, Rev. Phys. Appl. **12**, 1543 (1977).
[30]K. Shima, T. Ishihara, and T. Mikumo, Nucl. Instrum. Methods **200**, 605 (1982).
[31]E. Baron and B. Delaunay, Phys. Rev. A **12**, 40 (1975).
[32]J. A. Martin, R. L. Auble, K. A. Erb, *et al.*, Nucl. Instrum. Methods **A244**, 187 (1986).
[33]A. V. Belozerov, K. Borcha, I. Vintsour *et al.*, Communication R7-88-388 [in Russian], JINR, Dubna (1988).
[34]B. Franzke, Scientific Report GSI 83-1 (1982), p.162.
[35]M. Langevin and R. Anne, Preprint GANIL, pp. 84, 16.
[36]R. Bimbot, S. Della-Negra, P. Agyer *et al.*, Z. Phys. A **322**, 443 (1985).
[37]J. R. Rozet, A. Chetioui, R. Bouisett *et al.*, Phys. Rev. Lett. **58**, 337 (1987).
[38]K. Shima, T. Ishiara, T. Miyoshi, and T. Mikumo, Phys. Rev. A **28**, 2162 (1983).
[39]E. Baron, IEEE Trans. **NS-26**, 2411 (1979).
[40]Y. Baudinet-Robinet, Nucl. Instrum. Methods **190**, 197 (1981).
[41]K. Shima, T. Ishihara, and T. Mikumo, Nucl. Instrum. Methods **230(B2)**, 222 (1984).
[42]Y. Baudinet-Robinet, H. P. Garnir, P. D. Dumont *et al.*, Phys. Lett. **63A**, 19 (1977).
[43]Y. Baudinet-Robinet, Phys. Rev. A **26**, 62 (1982).
[44]C. D. Moak, H. O. Lutz, L. B. Bridwell *et al.*, Phys. Rev. **176**, 427 (1968); Phys. Rev. Lett. **18**, 41 (1967).
[45]L. Grodzins, R. Kalish, D. Murnick *et al.*, Phys. Lett. **24B**, 282 (1967).
[46]S. Datz, C. Moak, H. D. Lutz *et al.*, At. Data **2**, 273 (1971).
[47]N. Bohr and J. Lindhard, K. Dan. Vidensk. Selsk. Mat.-Fys. Medd. **28**, No. 7 (1954).
[48]H.-D. Betz and L. Grodzins, Phys. Rev. Lett. **25**, 211 (1970).
[49]S. Della-Negra, Y. Le Beyec, B. Monart *et al.*, Phys. Rev. Lett. **58**, 17 (1987).
[50]Y. Ryding, A. B. Wittkower, and P. H. Rose, Phys. Rev. A **3**, 1658 (1971).
[51]T. A. Carlson, W. E. Hunt, M. O. Krause *et al.*, Phys. Rev. **151**, 41 (1966).
[52]K. E. Stiebing, K. Bethge, H. Bokemeyer *et al.*, Scientific Report GSI 87-1 (1986), p. 172.
[53]D. Chmielewka, Z. Suikowski, R. V. F. Janssens *et* al., Nucl. Phys. **A366**, 142 (1981); H. Ernst, W. Hennig, and C. N. Davids, Phys. Lett. **119B**, 307 (1982).
[54]M. S. Freedmann, Ann. Rev. Nucl. Sci. **24**, 209 (1974).
[55]K. Bethge, A. Bösser, H. Bokemeyer *et al.*, Scientific Report GSI 01-87 (1987), p. 19.
[56]W. Wieclawick, R. Acad. Sci. **266**, 557 (1968).
[57]N. K. Skobelev, V. Z. Maidikov, G. S. Popeko *et al.*, Yad. Fiz. **29**, 615 (1979) [Sov. J. Nucl. Phys. **29**, 316 (1979)].
[58]N. K. Skobelev, in *Proceedings of the International Symposium on Nuclear Reactions, Balatonfüred, Hungary, June 1977,* edited by L. P. Csernai (Budapest, 1978), p. 319.
[59]M. Sowinski and N. K. Skobelev, Nukleonika **25**, 1001 (1980).
[60]V. Z. Maĭdikov, N. T. Surovitskaya, O. F. Nemets *et al.*, Preprint D7-80-556 [in Russian], JINR, Dubna (1980).
[61]V. Z. Maĭdikov, N. T. Surovitskaya, N. K. Skobelev, and O. F. Nemets, Yad. Fiz. **36**, 1103 (1982) [Sov. J. Nucl. Phys. **36**, 645 (1982)].
[62]N. K. Skobelev, V. Z. Maĭdikov, and N. T. Surovitskaya, Z. Phys. A **314**, 5 (1983).
[63]H. Wohlfarth, W. Lang, H. Dann *et al.*, Z. Phys. A **287**, 153 (1979).
[64]A. V. Belozerov, N. K. Skobelev, Yu. E. Penionzhkevich *et al.*, in *Heavy Ion Physics—85, Collected Abstracts,* Preprint R7-86-322 [in Russian], JINR, Dubna (1986), p. 54.
[65]N. K. Skobelev, D. V. Bugaev, V. Z. Maĭdikov, and N. T. Surovitskaya, in *Abstracts from the International School–Seminar on Heavy Ion Physics,* Preprint D7-86-434 [in Russian], JINR, Dubna (1986), p. 94.
[66]V. Z. Maĭdikov, in *Proceedings of the International Symposium on Ion-Beam Nuclear Spectroscopy, Debrecen, Hungary, May 1984,* edited by Zs. Dombradi and T. Fenyes (Academiai Klado, Budapest, 1984), Vol. 2, p. 477.
[67]D. V. Bugaev, V. Z. Maĭdikov, N. K. Skobelev, and N. T. Surovitskaya, in *Abstracts of the 37th Conference on Nuclear Spectroscopy and Nuclear Structure, Yurmala, April 1987* [in Russian] (Nauka, Leningrad, 1987), p. 257.
[68]D. Habs, V. Metag, H. J. Specht, and G. Ulfert, Phys. Rev Lett. **38**, 387 (1977); G. Ulfert, D. Habs, V. Metag *et al.* Nucl. Instrum. Methods **148**, 369 (1978).
[69]USSR Inventor's Certificate No. 708857: "An analyzer for nuclear reaction products" [in Russian], N. K. Skobelev and V. Z. Maĭdikov, OIPOTZ No. 30, 343 (1980).
[70]G. Münzenberg, W. Faust, F. R. Hessberger *et* al, Nucl. Instrum. Methods **186**, 424 (1981).
[71]A. V. Yeremin, A. N. Andreyev, D. D. Bogdanov *et al.*, Preprint E15-88-137, JINR, Dubna (1988).
[72]N. Stolterfoht, D. Schneider, D. Burch *et* al., Phys. Rev. Lett. **33**, 59 (1974).
[73]S. Schmidt, C. Kelbch, G. Kraft *et al.*, Scientific Report GSI-1987, GSI 88-1 (1988), p. 184.
[74]C. Kozhuharov, in *Quantum Electrodynamics of Strong Fields,* edited by W. Greiner (Plenum, New York, 1983), p. 317.
[75]H. W. Schnopper, H.-D. Betz, J. P. Delvaille *et al.*, Phys. Rev. Lett. **29**, 898 (1972).
[76]W. Meyehof, Phys. Rev. Lett. **30**, 1279 (1973); **32**, 1279 (1974).
[77]W. Frank, P. Gippner, K.-H. Kaun *et al.*, Phys. Lett. **59B**, 41 (1975); K.-G. Kaun, in *Proceedings of the International School–Seminar on Heavy Ion Interactions with Nuclei and the Synthesis of New Elements* Dubna 1975); Preprint D7-9734 [in Russian], JINR, Dubna (1976), p. 245.
[78]E. S. Parilis, in *Proceedings of the Sixth International Conference on the*

Physics of Electronic and Atomic Collisions (Cambridge, 1969), p. 835.
[79]H. Geissel, Y. Laichter, W. F. W. Schneider, and P. Armbruster, Nucl. Instrum. Methods **215**, 329 (1983).
[80]H. Geissel, Y. Laichter, W. F. W. Schneider, and P. Armbruster, Nucl. Instrum. Methods **194**, 21 (1982).
[81]H. Geissel, Y. Laichter, W. F. W. Schneider, and P. Armbruster, Phys. Lett. **99A**, 77 (1983).
[82]R. Bimbot, H. Gauvin, and I. Orliange, Nucl. Instrum. Methods **B17**, 1 (1986).
[83]J. F. Ziegler, *Handbook of Stopping Cross Sections for Energetic Ions in All Elements* (Pergamon Press, New York, 1980).

Translated by Patricia Millard